EBioMedicine 4 (2016) 104–114

Contents lists available at ScienceDirect

EBioMedicine

journal homepage: www.ebiomedicine.com

Research Paper

Adjunctive Phosphodiesterase-4 Inhibitor Therapy Improves Antibiotic Response to Pulmonary Tuberculosis in a Rabbit Model

Selvakumar Subbian [a,*], Liana Tsenova [a,b], Jennifer Holloway [c,1], Blas Peixoto [a,1], Paul O'Brien [a,1], Véronique Dartois [a], Vikram Khetani [d], Jerome B. Zeldis [d], Gilla Kaplan [a,2]

[a] Public Health Research Institute (PHRI) of Rutgers Biomedical and Health Sciences (RBHS), Newark, NJ, USA
[b] Department of Biological Sciences, NYC College of Technology, Brooklyn, NY, USA
[c] Department of Pharmaceutics, Ernest Mario School of Pharmacy, Rutgers University, Piscataway, NJ, USA
[d] Celgene Corporation, Summit, NJ, USA

ARTICLE INFO

Article history:
Received 5 August 2015
Received in revised form 6 January 2016
Accepted 11 January 2016
Available online 14 January 2016

Keywords:
Pulmonary tuberculosis
Immune modulation
Phosphodiesterase inhibitor
Lung fibrosis
Inflammation

ABSTRACT

Objectives: Adjunctive host-directed therapy is emerging as a new potential approach to improve the outcome of conventional antimicrobial treatment for tuberculosis (TB). We tested the ability of a phosphodiesterase-4 inhibitor (PDE4i) CC-11050, co-administered with the first-line anti-TB drug isoniazid (INH), to accelerate bacillary killing and reduce chronic inflammation in the lungs of rabbits with experimental *Mycobacterium tuberculosis* (Mtb) infection.

Methods: A rabbit model of pulmonary TB that recapitulates the pathologic manifestations seen in humans was used. Rabbits were infected with virulent Mtb by aerosol exposure and treated for eight weeks with INH with or without CC-11050, starting at four weeks post infection. The effect of CC-11050 treatment on disease severity, pathology, bacillary load, T cell proliferation and global lung transcriptome profiles were analyzed.

Results: Significant improvement in bacillary clearance and reduced lung pathology and fibrosis were noted in the rabbits treated for eight weeks with INH + CC-11050, compared to those treated with INH or CC-11050 only. In addition, expression of host genes associated with tissue remodeling, tumor necrosis factor alpha (TNF-α) regulation, macrophage activation and lung inflammation networks was dampened in CC-11050-treated, compared to the untreated rabbits.

Conclusions: Adjunctive CC-11050 therapy significantly improves the response of rabbits with experimental pulmonary TB to INH treatment. We propose that CC-11050 may be a promising candidate for host directed therapy of patients with pulmonary TB, reducing the duration and improving clinical outcome of antibiotic treatment.

1. Introduction

Tuberculosis (TB), caused by *Mycobacterium tuberculosis* (Mtb) is a common infectious disease among humans, accounting for 9 million new cases and 1.5 million deaths in 2013 (http://www.who.int/tb/publications/factsheet_global.pdf?ua=1). The current anti-TB drug regimen used for directly observed therapy, short course (DOTS) is ineffective at completely eliminating the infecting Mtb and disease associated lung pathology (Mitchison, 2000; Sirgel et al., 2000). Since most of the antibiotics currently in use for TB treatment under DOTS primarily target actively growing Mtb, non- or slow replicating and dormant bacilli, present in the granulomas of active TB cases, are not efficiently killed (Mitchison, 2000; Zhang et al., 2012). Such dormant bacillary population can resume growth and cause symptomatic, active disease in the infected host in response to conditions that suppress immunity (Cardona, 2010; Ehlers, 2009). Moreover, after successful completion of DOTS therapy, lung function and quality of life of TB patients can be significantly compromised by the fibrotic scars and irreversible tissue damage, rendering them more susceptible to recurrent TB disease and other pulmonary infections (den Boon et al., 2008; Verver et al., 2005). Therefore, alternate approaches for better bacterial elimination and treatment outcome are urgently needed to control the TB epidemic and improve the quality of life of TB patients after treatment (Zumla et al., 2014).

Progression of initial pulmonary Mtb infection to chronic active TB versus establishment of latent Mtb infection (LTBI) involves a shift in the regulation of inflammatory responses of host immune cells (Dorhoi & Kaufmann, 2014; Behar et al., 2014). During progressive pulmonary TB, the onset of early and exacerbated inflammation, associated with tissue necrosis and cavity formation impairs host resistance

* Corresponding author at: Laboratory of Mycobacterial Immunity and Pathogenesis, 225 Warren Street, Room W250.Q, Newark, NJ 07103, USA.
E-mail address: subbiase@njms.rutgers.edu (S. Subbian).
[1] These authors contributed equally.
[2] Present address: Bill and Melinda Gates Foundation, Seattle, WA, USA.

http://dx.doi.org/10.1016/j.ebiom.2016.01.015

and, promotes dissemination of Mtb within and outside the lung (Kaufmann & Dorhoi, 2013; Sugawara, 2009). Disease pathology during Mtb infection is driven by reactive oxygen and nitrogen species as well as cytokines, chemokines and other inflammatory mediators such as TNF-α, interferon gamma-induced protein 10 (IP-10) and C-reactive protein (CRP) produced by activated macrophages, neutrophils and other immune cells (Kaufmann & Dorhoi, 2013; Schlesinger, 1996). The mycobacterial population thriving in an elevated host inflammatory environment adapts to a dormant phenotype with slow or no replication that is refractory to antibiotic killing (Chao & Rubin, 2010). Thus, adjunctive host targeted immune therapies that improve disease pathology by modulating the inflammatory response to Mtb infection and that shorten the duration of standard antibiotic treatment by increasing macrophage anti-microbial activity, is an important emerging concept in treatment of TB (Wallis & Hafner, 2015; Hawn et al., 2015). Phosphodiesterases (PDE) are enzymes that hydrolyze cyclic nucleotides, such as cyclic adenosine and guanosine monophosphates (cAMP and cGMP) (Francis et al., 2011; Conti et al., 2003). In higher mammals at least 11 different PDEs (PDE1–PDE11) have been reported; many are implicated in modulating host cell functions, including cytokine and chemokine produced in response to various diseases (Keravis & Lugnier, 2012; Bender & Beavo, 2006). PDE4 is a cAMP-specific hydrolase present predominantly in host leukocytes, including macrophages, neutrophils and lymphocytes (Spina, 2003; Houslay et al., 1998). Since accumulation of cAMP, through blocking its hydrolysis, negatively regulates inflammation, several PDE4is have been tested and found to be useful for treating human inflammatory diseases including asthma and psoriasis (Spina, 2003; Azam & Tripuraneni, 2014; Maurice et al., 2014). Over the past several years, we have investigated the therapeutic effects of the immune modulatory drugs (IMiDs®), PDE4i, and other small molecules as adjunctive therapies with anti-TB antibiotics in different animal models (Moreira et al., 1997; Tsenova et al., 2002; Koo et al., 2011; Subbian et al., 2011a; Subbian et al., 2011b). Our central hypothesis is that reducing but not fully blocking TNF-α production by host cells would alleviate inflammatory responses and improve the outcome of antibiotic treatment during Mtb infection. Recently, we showed that treatment with the PDE4i CC-3052, together with INH, significantly reduced Mtb growth and disease pathology in murine and rabbit models of pulmonary TB (Koo et al., 2011; Subbian et al., 2011a; Subbian et al., 2011b). In the present study, we report the "proof-of-concept" for the activity of another PDE4i (CC-11050) with improved therapeutic properties. Moreover, CC-11050 has an investigational new drug (IND) application and has been in clinical trials for other indications. We chose INH, since this drug predominantly kills actively replicating bacteria and ineffective in killing against dormant bacilli. In addition, INH monotherapy has been used as a prophylactic treatment against reactivation of latent Mtb infection in humans. Our results show that CC-11050 dampens infection-induced inflammation and improves bacterial clearance as well as clinical outcome in INH treated rabbits with pulmonary TB. The present work confirmed that PDE4 inhibition with CC-11050 gives similar effects as CC-3052 and other PDE4is. Results from this study will serve as a proof of concept to guide a human clinical trial that will be conducted soon (JBZ personal communication).

2. Materials and Methods

2.1. Bacterial Culture and Chemicals

M. tuberculosis HN878 (a strain of W-Beijing lineage) was grown to mid-log phase (OD_{600} = 0.5–0.7) in Middlebrook 7H9 media containing 0.5% glycerol, 0.25% Tween 80 and 10% oleic acid dextrose catalase (OADC) supplement (BD Biosciences, MD) and aliquots were stored at −80 °C. The bacterial inoculum for rabbit aerosol infection was prepared as described previously (Subbian et al., 2011c). Ketamine, acepromazine and euthasol used to sedate and euthanize rabbits were purchased from Henry Schein Animal Health, OH. CC-11050 was supplied by Celgene Corporation, NJ. All other chemicals were purchased from Sigma-Aldrich (Sigma-Aldrich, MO), unless mentioned otherwise.

2.2. Animal Welfare and Ethical Statement

Specific pathogen free, female New Zealand white rabbits (Millbrook Farms, MA) of 2.3 to 2.6 kg body weight were used in this study. Each rabbit was housed individually without any restriction on food and water consumption (ad libitum) and was handled humanely according to the United States Department of Agriculture (USDA) policies. All the procedures with Mtb-infected rabbits, including infection, gavage, post-infection and treatment monitoring were performed in bio safety level-3 facilities according to the protocols approved by the Institutional Animal Care and Use Committee (IACUC) of the Rutgers University and were in compliance with institutional, national and international guidelines governing the use of experimental animals.

2.3. Pharmacokinetics of CC-11050

2.3.1. Structure of CC-11050

CC-11050 (N-[2-[(1S)-1-(3-ethoxy-4-methoxyphenyl)-2-(methylsulfonyl) ethyl]-2,3-dihydro-3-oxo-1H-isoindol-4-yl]-(9Cl) cyclopropanecarboxamide) is a PDE4i with anti-inflammatory activities. CC-11050 has an empirical formula of $C_{24}H_{28}N_2O_6S$ with one chiral center in its structure (Supplementary Fig. 1A).

2.3.2. Sample Collection

Uninfected rabbits were divided into two experimental groups (n = 3 per group) and treated by oral gavage with either 25 mg per kg or 50 mg per kg of CC-11050. Venous blood was collected in vacutainer tubes (BD & Co, NJ) at time 0 (pre-treatment), 15 min, 30 min, 1 h, 2 h, 4 h, 8 h, and 24 h after a single gavage administration of CC-11050. In another experiment, groups of rabbits (n = 3 per group) were treated by oral gavage with CC-11050 at 25 or 50 mg per kg per day for four days and blood was collected as before. Plasma was collected after centrifuging the blood samples at 1100 ×*g* for 10 min. To determine whether INH and CC-11050 interact with each other in the Mtb-infected rabbits, blood samples were collected after 2 weeks of treatment and plasma was collected as mentioned above for liquid chromatography–mass spectrometry (LC–MS) analysis.

2.3.3. Bioanalytical Method for CC-11050

The standard curve (1 to 4000 ng per ml) and quality control samples (3 to 3200 ng per ml) were prepared by diluting 1 mg per ml stock CC-11050 solution in rabbit plasma diluted 1:1 with Sorenson's citrate buffer (25 mM; pH 1.5). The internal working standard solution (25 ng per ml) was prepared by diluting 1 mg per ml internal standard stock solution of $^{13}CD_3$–CC-11050. Briefly, 100 μl of the working internal standard solution was added to 25 μl of each standard, quality control or test samples, and mixed well. After centrifugation at 4000 rpm for 10 min, 75 μl of the supernatant was transferred to a clean 96-well plate for analysis. Samples were analyzed by LC–MS using a Sciex API 4000 Triple Quadrupole Mass Spectrometer (Sciex, Division of MDS Inc., Canada) coupled to a Shimadzu HPLC System (Shimadzu Scientific Instruments, MD) with a Phenomenex Gemini column (5 μm, 2.0 × 50 mm) (Phenomenex, CA). Samples were analyzed using the following chromatographic conditions: mobile phase A consisted of 0.1% formic acid in water and mobile phase B consisted of 0.1% formic acid in acetonitrile. The gradient conditions were: 0 min for 10% B, 0.0–2.0 min from 10% B to 75% B, 2.1–3.0 min for 95% B, and 3.05–4.0 min for 10% B. A positive ion mode with turbo spray, an ion source temperature of 450 °C, and a dwell time of 100 ms were utilized for mass spectrometric detection. Quantification of analytes was performed using multiple reactions monitoring (MRM) at the following transitions: *m/z* 473.1 to *m/z* 178.1 and *m/z* 477.1 to *m/z* 182.1 for CC-11050

and its internal standard, respectively. Quadratic regression plots of peak area ratios of analyte to its internal standard versus analyte concentration were derived with $1/x^2$ weighting. Pharmacokinetic parameters were calculated using Watson LIMS™ (version 7.4, Thermo Fisher, PA). The maximum plasma concentration (C_{max}) and the corresponding time (T_{max}) were determined from actual data. The area under the plasma concentration-time curve from time 0 to the last measurable time point (AUC_{last}) was determined using the linear and linear-log trapezoidal rule of non-compartmental model. Nominal times were used for pharmacokinetic parameter calculations. All statistics were calculated by Watson LIMS™. Plasma concentrations below the limit of quantitation (BLOQ) were treated as zero for calculation.

2.4. Pulmonary Mtb Infection of Rabbits

Seventy rabbits (n = 71) were used for aerosol infection with Mtb HN878 in a "snout-only" exposure system (CH Technologies Inc., NJ) as reported earlier (Tsenova et al., 2006). After one week of acclimatization, rabbits were sedated and exposed to Mtb-containing aerosols through individual, "snout-only" apparatus. The bacterial inoculum was standardized to deliver approximately 3.3 $\log_{10}$ bacterial colony forming units (CFU). To determine the actual number of CFU implanted, a group of aerosol-exposed rabbits (n = 10) was euthanized after 3 h (T = 0) and their lung homogenates were plated on Middlebrook 7H11 agar plates (Difco Laboratories Inc., Detroit, MI). Bacterial CFU were enumerated from these plates after 4–6 weeks of incubation at 37 °C. Similarly, CFU were calculated from six animals (n = 6) at 4 weeks post-infection (i.e., at the onset of treatment). Starting at 4 weeks post-infection, group of Mtb-infected rabbits was treated by oral gavage with CC-11050 (50 mg per kg) or INH (50 mg per kg) or a mixture of INH + CC-11050 five days a week for 8 weeks (i.e., until 12 weeks post-infection); a group of Mtb-infected rabbits (n = 7) was left untreated as control. The treatment compounds were dissolved in water before oral gavage using a flexible rubber catheter with a lubricant. At 8 and 12 weeks post-infection, Mtb-infected rabbits from all four groups (n = 6–8 per group per time point) were euthanized and the lung, liver and spleen were harvested aseptically and processed immediately to prepare homogenates in sterile saline for CFU assay. Representative portions of these organs were also stored in formalin for histopathologic analysis or frozen immediately for total RNA isolation. To monitor disease severity, weight of total body, lung, liver and spleen was measured and number of sub-pleural lung granulomas was counted for all the infected rabbits at each experimental time point.

2.5. Mycobacterial Drug Susceptibility Test

Bacterial resistance to INH was tested by plating serial dilutions of lung homogenates on 7H10 agar media containing 0.2 or 1 μg per ml of INH. In addition, susceptibility of Mtb strains to INH (0.0125 μg per ml or 0.2 μg per ml) with or without CC-11050 (5, 50 and 250 mM) were tested in vitro using liquid cultures. Briefly, about 6 $\log_{10}$ CFU per ml of Mtb was incubated with or without INH and CC-11050. At 24, 48 and 72 h post-treatment, samples were serially diluted and plated on 7H10 agar media. Colonies were enumerated after 3 weeks of incubation at 37 °C.

2.6. Histology and Morphometry

Formalin-fixed lung tissue sections from Mtb-infected rabbits were stained with hematoxylin and eosin (H&E) to visualize cellular composition or with Ziehl–Neelsen acid fast staining (AFB) to visualize Mtb (IDEXX-RADIL Laboratories Inc., MO). Masson's trichrome staining was performed to examine collagen deposition and fibrosis as previously described (Subbian et al., 2012). Stained lung sections were analyzed and photographed using a Nikon Microphot-FX photomicrographic system with NIS-Elements F3.0 software (Nikon Instruments Inc., NY). Semi quantitative evaluation of pathology was based on the following scoring system: 0—intact lung; 1—increased cellularity; 2—granuloma formation; 3—granulomas with central necrosis; 4—large coalescent lesions with necrosis; 5—partial liquefaction; 6—extensive liquefaction; 7—cavity. Similarly, the extent of fibrosis was scored using modified Ashcroft scale: 0—normal lung (no fibrosis); 1—minimal fibrous thickening of alveolar or bronchiolar vessels; 2—moderate thickening of walls without obvious damage to lung architecture; 3—Increased fibrosis with definite damage to lung structure and formation of fibrous bands or small fibrous masses; 4—large fibrous areas; 5—total fibrous obliteration of the field (Hubner et al., 2008; Robbe et al., 2015). The number and size of granulomatous lesions in the Mtb-infected rabbit lung sections were enumerated by morphometric measurements using Sigmascan Pro software (Systat Softwares, Inc., CA).

2.7. Flow Cytometric Analysis

Single cell suspensions were prepared from rabbit spleen and used for flow cytometry as described previously (Subbian et al., 2011c). Briefly, spleenocytes were stained with CFSE (Life Technologies, Carlsbad, CA) and stimulated with concanavalin A (ConA) or heat-killed Mtb or purified protein derivative (PPD) or left untreated. Cells were stained primarily with anti-rabbit CD4 or anti-rabbit CD8 antibodies followed by APC anti-mouse IgG (BD Biosciences, San Jose, CA). The samples were processed through FACSCalibur flow cytometer (BD Biosciences, San Jose, CA) and data was analyzed using FlowJo software (Tree Star, Ashland, OR).

2.8. RNA Isolation and Microarray Analysis

Total RNA from rabbit lungs was isolated using TRIzol reagent (Invitrogen, CA) as described previously (Subbian et al., 2013a). Portions of the lung tissue were homogenized with TRIzol, extracted with chloroform and purified using NucleoSpin RNA II kit (Macherey-Nagal, GmbH). The quality and quantity of purified RNA was estimated using Nanodrop (NanoDrop Products, DE). One microgram of total RNA from each rabbit lung was processed separately for cDNA synthesis using a SuperScript II system (Agilent Technologies, CA). cDNA from three rabbits per group was processed independently for microarray experiments as described earlier (Subbian et al., 2013a). The 4x44k rabbit microarray slide and associated reagents were obtained from Agilent Technologies (Agilent Technologies, CA). Synthesis of cDNA, labeling, hybridization and post-hybridization washings were performed according to the established, standardized protocols of the Center for Applied Genomics (http://www.cag.icph.org/index.htm) of Rutgers University. The slides were scanned and background-corrected probe intensity was extracted using the Agilent Scanner and Feature Extraction Software (Agilent Technologies, CA), respectively. Normalized data from individual rabbits treated with CC-11050 or INH or INH + CC-11050 (n = 3 per group) were pooled respectively and compared to the pooled data (n = 3) from the untreated but Mtb-infected control group. One-way ANOVA followed by Bonferroni's test was performed in Partek Genomics Suite, version 6.5 (Partek Inc., MO) and was used to compare multiple experimental groups and treatment time. A false discovery rate of less than 5% (FDR < 5%) was used as cut-off to identify the statistically significantly differentially expressed genes (SDEG) in each of the treatment groups, relative to untreated controls. The list of SDEG was loaded into QIAGEN's Ingenuity® Pathway Analysis (IPA®-QIAGEN, CA) to determine significantly enriched (P < 0.05; right-tailed Fisher's Exact Test) biological functions, networks and canonical pathways as described previously (Subbian et al., 2013b). The microarray data has been submitted to Gene Expression Omnibus (GEO), accession number GSE74687.

2.9. Quantitative PCR (qPCR) Analysis

Total RNA from Mtb-infected rabbit lungs was reverse transcribed using a Sprint RT system following manufacturer instructions (Clontech, CA) and used in qPCR as described before (Subbian et al., 2011a). Five nanograms of cDNA was mixed with gene-specific primer pair and 2xSYBR green master mix; ROX dye was included as internal control and the reaction was set up as recommended by the manufacturer (Takara, CA). Host GAPDH gene was used as internal control in all tested samples. The qPCR was performed in a Strategene Mx3005p instrument and the data was analyzed using MxPro Software (Agilent Technologies, CA) to determine threshold cycle (Ct). Change in gene expression was calculated using the formula $2^{-\Delta Ct}$, where ΔCt is the difference in Ct between target gene and GAPDH. Nucleotide sequence of gene specific primers used in this study is shown in Supplementary Table 1.

2.10. Statistical Analysis

The microarray data was analyzed by ANOVA using Partek Genomics Suite, version 6.5 (Partek Inc., MO) to select significantly differentially expressed genes (SDEG) as reported earlier (Subbian et al., 2013b). Students' *t*-test from Microsoft Excel 2007 and GraphPad Prism software (GraphPad Software, CA) was used to compare pair-wise significance for the bacterial CFU assay, pathologic analysis, T-cell proliferation assay and qPCR experiments. For all experiments $P < 0.05$ was considered statistically significant.

3. Results

3.1. Pharmacokinetics of CC-11050

Peak plasma concentrations were reached between 4 and 8 h (T_{max}) following single or multiple 25 and 50 mg per kg doses of CC-11050 (Supplementary Fig. 1). There were no significant differences observed in the maximum concentrations (C_{max}) reached at T_{max} after one day or 4 days of oral dosing within the 25 mg per kg per day or 50 mg per kg per day dose groups (Supplementary Table 2a). The mean exposures calculated from the area under the concentration curve ($AUC_{[0-24]}$) increased proportionately to the dose on both day 1 and day 4. In addition, about a two-fold increase in mean CC-11050 accumulation was observed at both dose levels (Supplementary Table 2a). As shown in Supplementary Table 2b and Supplementary Fig. 2, the plasma concentration of INH was not affected by co-administration of CC-11050.

3.2. Adjunctive CC-11050 Treatment With INH Significantly Reduces Tissue Bacillary Loads

To determine the efficacy of CC-11050 at improving the antimicrobial activity of the TB drug INH, we measured the number of CFU in the lung, liver and spleen of aerosol infected rabbits at various time points post-exposure or treatment (Fig. 1a). About 3.3 $\log_{10}$ CFU of Mtb HN878 implanted in rabbit lungs on day 0 (3 h post-infection), proliferated to about 7 $\log_{10}$ CFU after 4 weeks (Fig. 1b and Supplementary Table 3). In the untreated rabbits the bacillary load remained high at 8 weeks (mean = 6.6 $\log_{10}$) and 12 weeks (mean = 6.2 $\log_{10}$) post-infection. Treatment with CC-11050 alone for 4 weeks or 8 weeks (8 weeks or 12 weeks post-infection) did not affect the number of CFU significantly compared to the untreated rabbits ($P = 0.949$ and 0.073, respectively), suggesting that CC-11050 does not have any inherent anti-mycobacterial activity. Treatment of Mtb-infected rabbits with INH alone for 4 weeks moderately reduced the lung bacillary load; however, after 8 weeks of treatment a significant reduction in the number of CFU was noted ($P = 0.0223$), compared to the untreated animals (Fig. 1b). There was no significant difference in CFU between CC-11050-treated and INH treated rabbits after 4 weeks ($P = 0.562$) or 8 weeks ($P = 0.39$) of treatment (i.e., 8 and 12 weeks post infection).Treatment of Mtb-infected rabbits with INH + CC-11050 for 4 weeks reduced the lung bacillary load but this effect was not statistically significant, compared to the other groups. However, a significant reduction in the lung bacillary load was observed after

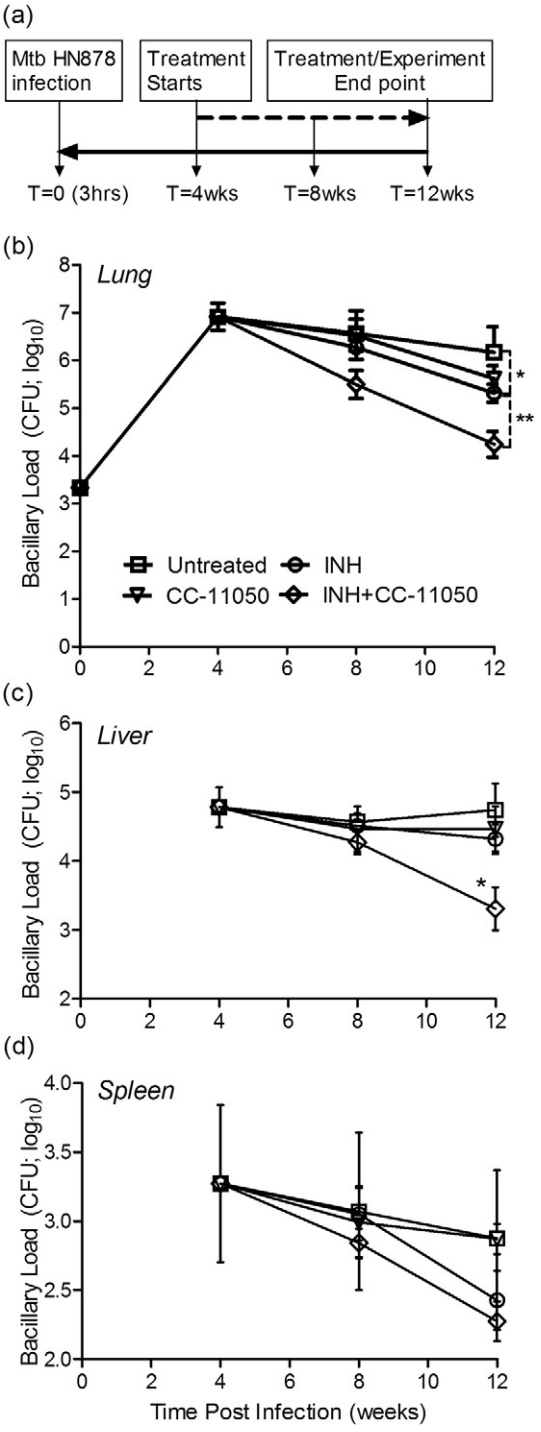

Fig. 1. Experimental design and bacillary load in the lung, liver and spleen of Mtb-infected rabbits. (a) Schema of experimental design showing rabbit infection, treatment and necropsy time points. (b) Kinetics of bacillary growth in the lungs of Mtb-infected rabbits with or without CC-11050, INH or INH + CC-11050 treatment. *P = 0.0223 at 12 weeks between untreated and INH-treated animals. **P = 0.006 at 12 weeks between untreated and INH + CC-11050 treated animals. (c) Kinetics of bacillary burden in the liver of Mtb-infected rabbits with or without CC-11050, INH or INH + CC-11050 treatment. *P = 0.002 at 12 weeks between untreated and INH + CC-11050 treated animals. (d). Kinetics of bacillary load in the spleen of Mtb-infected rabbits with or without CC-11050, INH or INH + CC-11050 treatment. Values plotted are mean and standard deviation from 6 to 10 rabbits per group per time point.

8 weeks of INH + CC-11050 treatment, compared to the untreated (P = 0.006) or INH alone treated (P = 0.0055) animals (Fig. 1b). At these time points, significant difference was noted between the CC-11050-treated and CC-11050 + INH treated rabbits (P = 0.043 for 4 weeks and P = 0.006 for 8 weeks of treatment). This observation suggests that immune modulation with CC-11050 can improve INH-mediated killing of Mtb in the rabbit lungs. It is important to note that when CC-11050 was used alone, the bacillary growth did not increase, as seen when the host immune response is inhibited (i.e., immune suppression). Tubercle bacilli were also recovered in significant numbers from the livers and spleens of all infected animals at 4 weeks post infection (Fig. 1c and 1d), suggesting bacillary dissemination from the lungs. A significant reduction in the liver bacterial load was noted only in rabbits treated with INH + CC-11050 for 8 weeks. In the spleen, the lowest number of CFU was also observed in the same treatment group.

3.3. CC-11050 Treatment Did Not Affect the Bacterial Susceptibility to INH

To determine whether CC-11050 affect Mtb susceptibility to INH, we performed CFU assay using lung homogenates of rabbits treated with CC-11050 with or without INH. No significant difference was observed in the number of CFU obtained between INH and INH plus CC-treated samples (data not shown). In addition, in vitro INH susceptibility testing of Mtb with or without CC-11050 did not show significant difference between these two groups (Supplementary Fig. 3).

3.4. CC-11050 Plus INH Treatment Dampens Disease Burden

To estimate the overall disease burden of Mtb-infected rabbits with or without any treatment, net weight of the lung, liver and spleen was measured after 4 or 8 weeks post-treatment (Supplementary Fig. 4). No significant difference in the weights of these organs was noted between the untreated rabbits and those treated with CC-11050 or INH with or without CC-11050.

To evaluate the development of granulomas over time, whole rabbit lungs from all groups of the Mtb-infected (treated or untreated) animals were examined for gross pathology at the end of treatment (12 weeks post-infection) (Fig. 2a and h). The lesions in the untreated (Fig. 2a and e) and CC-11050-alone treated (Fig. 2b and f) rabbits appeared larger than those noted in the other treatment groups. Although INH alone-treated animals had smaller visible lesions at 4 or 8 weeks of treatment (Fig. 2c and g), the smallest lesions were observed in the lungs of rabbits treated with INH + CC-11050 at these times (Fig. 2d and h). In the combination therapy group, most of the lung parenchyma appeared normal and unlike the other groups, a number of the lung sections had no lesions at all.

The total number of sub-pleural lesions counted in both lungs of untreated Mtb-infected rabbits was about 80 at 4 weeks post-infection. This number did not change significantly at 12 weeks post-infection in the untreated, the CC-11050 alone- or INH alone-treated animals (Fig. 2i). In contrast, rabbits treated for 8 weeks with INH + CC-11050 had a significantly lower number of visible sub pleural lesions, compared to the other groups (P < 0.0001) (Fig. 2i).

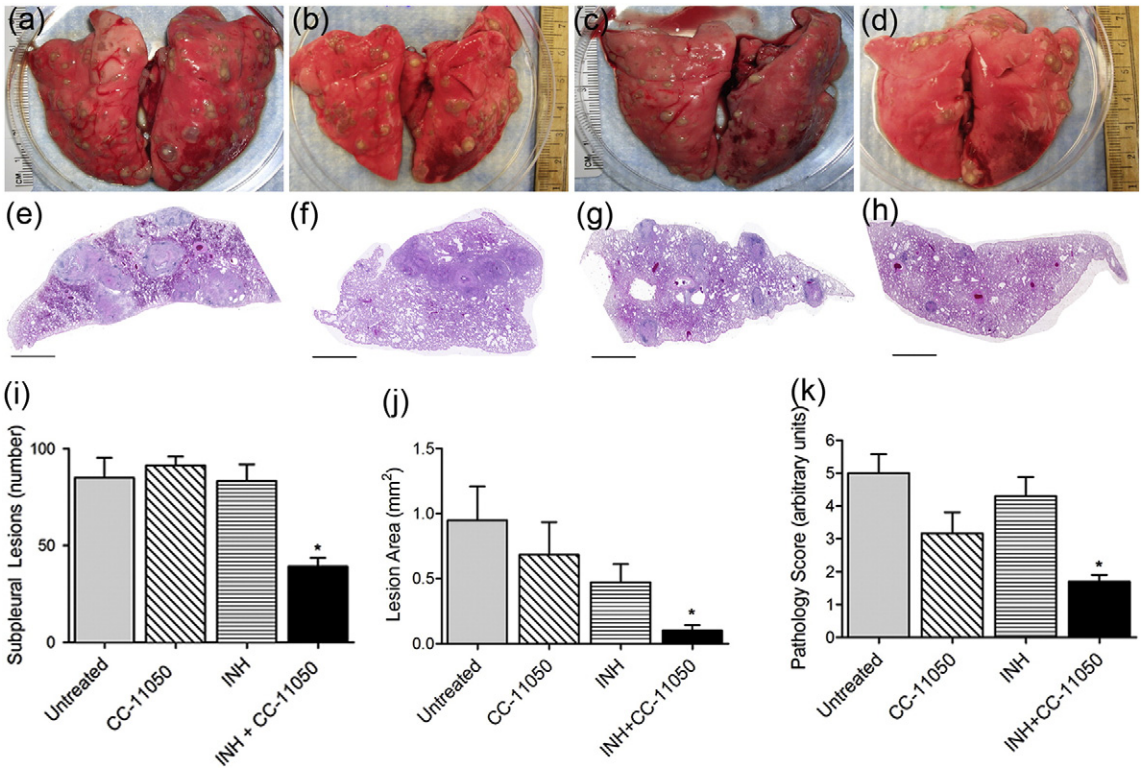

Fig. 2. Gross pathology and disease characteristics of Mtb-infected rabbit lungs. (a–d) Representative gross lung pathology images of Mtb-infected untreated (a), CC-11050- (b), INH- (c) or INH + CC-11050- (d) treated rabbits showing the distribution of dorsal sub-pleural granulomas at 12 weeks post-infection (8 weeks treatment). (e–h) Representative low magnification images of rabbit lung sections at 12 weeks post-infection, stained with hematoxylin & eosin, showing the general architecture of granulomas in Mtb-infected untreated (e), CC-11050- (f), INH (g) or INH + CC-11050 (h) treated rabbits. Scale bar = 1 mm. (i) Number of sub-pleural lung granulomas in Mtb-infected untreated or CC-11050 or INH or INH + CC-11050 treated rabbits at 12 weeks post-infection. Values plotted are average and standard deviation from 6 to 8 animals per group. *P = 0.0003 between untreated and INH + CC-11050 treated animals. (j) Area of lung granulomas in Mtb-infected untreated, CC-11050-, INH- or INH + CC-11050 treated rabbits at 12 weeks post-infection. Values plotted are average and standard deviation from 3 sections per animal; 6–8 animals per group. *P = 0.013 between untreated and INH + CC-11050 treated animals. (k) Pathology score of Mtb-infected untreated, CC-11050-, INH- or INH + CC-11050 treated rabbits at 12 weeks post-infection. Values plotted are average and standard deviation from 6 to 8 animals per group. *P = 0.04 between untreated and INH + CC-11050 treated animals.

Morphometric analysis of the histologic sections of lung tissue revealed significant differences in the size of the lesions (Fig. 2j). In the untreated animals, the granulomas at 12 weeks post-infection reached about 1 mm^2. No significant difference in the lesion area was noted between the untreated and CC-11050- or INH-alone treated animals, although the latter group had moderately reduced lesion size. Importantly, the greatest reduction in granuloma size was noted in the lungs of INH + CC-11050 treated rabbits (average = 0.102 mm^2) which was significantly lower compared to the untreated ($P = 0.013$) or INH-alone treated ($P = 0.040$) animals at 12 weeks post-infection (Fig. 2j).

To determine the extent of disease manifestations in the lungs, we scored the pulmonary pathology at the end of treatment (Fig. 2k). The untreated and INH-alone treated group had the highest disease complications, followed by the CC-11050 treated rabbits that showed a moderately reduced disease at 12 weeks post infection. In contrast, significant reduction ($P = 0.04$) in disease pathology was observed at this time in the INH + CC-11050 treated, compared to the untreated rabbits (Fig. 2k).

3.5. CC-11050 Plus INH Treatment Alleviates Lung Necrosis and Tissue Damage

Detailed, higher magnification histologic examination of the Mtb-infected rabbit lungs at 4 weeks showed multiple, well organized granulomas (size 0.5–1.5 mm diameter), some of which had initial central necrosis (not shown). At 12 weeks, untreated rabbits had multiple coalescent lesions with extensive necrosis, surrounded by macrophages and many lymphocytes (Fig. 3a and b). In some granulomas, mineralization (calcification) was seen. Polymorphonuclear leukocytes (PMNs) were observed at the border of the necrotic areas. Animals treated with CC-11050 alone, at 12 weeks post-infection (8 weeks of treatment), had similar large necrotic lesions (Fig. 3d and e), containing multiple epithelioid macrophages and less lymphocytes. INH-treated

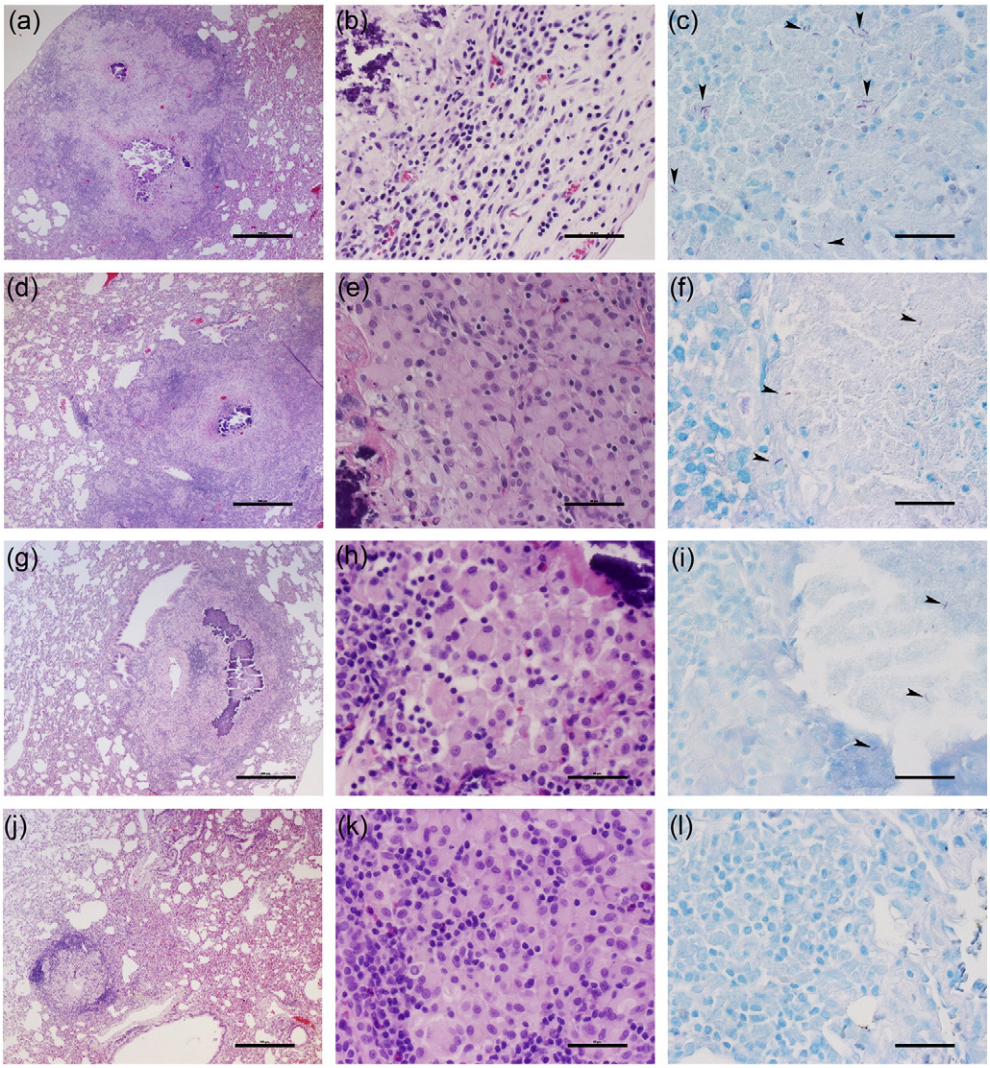

Fig. 3. Histopathology of Mtb-infected rabbit lungs 12 weeks post infection (8 weeks of treatment). (a, b and c) Representative images of H&E (a and b) or AFB (c) stained lung section from untreated rabbits. Well demarcated, large confluent granulomas with central necrosis and mineralization, surrounded by macrophages and many lymphocytes can be seen. High numbers of acid-fast bacilli (arrowheads) were also found in these granulomas. (d, e and f) Representative images of H&E (d and e) or AFB (f) stained lung section from rabbits treated with CC-11050 only. Well demarcated, large lesions with central necrosis surrounded by multiple epithelioid macrophages and less lymphocytes can be seen. Very few acid-fast bacilli are noted in these granulomas. (g, h and i) Representative images of H&E (g and h) or AFB (i) stained lung section from rabbits treated with INH only. Granulomas with central area of extensive necrosis and mineralization, surrounded by foamy macrophages and lymphocytes can be seen. Very few AFB-positive organisms were found in these granulomas. (j, k and l) Representative images of H&E (j and k) or AFB (l) stained lung section from rabbits treated with the combination of INH and CC-11050. Very few, well demarcated, non-necrotic small granulomas, undergoing resorption can be seen. No clearly visible AFB-positive organisms were observed in these granulomas. Figures a, d, g and j were photographed at 4× (Scale bar = 500 μm) and b, e, h and k at 40× (Scale bar = 50 μm) magnification, respectively. Sections c, f, i and l (acid-fast stain) were photographed at 80× (Scale bar = 25 μm) magnifications.

rabbits had a similar number of somewhat smaller lesions, compared to the untreated animals. The granulomas contained central area of necrosis and mineralization, surrounded by foamy macrophages and lymphocytes in the periphery (Fig. 3g and h). In contrast, significantly fewer and smaller granulomas (<0.5 mm diameter) were present in the INH + CC-11050 treated rabbits relative to the controls and other treatment groups (Fig. 3j and k). Most of the lesions were in the process of undergoing resorption and had no central necrosis. These observations were confirmed by a semi quantitative evaluation of lung pathology (see Section 2). The average disease score for animals treated with INH + CC-11050 was significantly lower than the control group and rabbits treated with INH alone (1.7 vs. 5 and 4.3 respectively; P = 0.0006 and 0.003 respectively). Acid-fast staining revealed numerous bacilli, mostly intracellular in the lesions from the control untreated rabbits (Fig. 3c). Few single AFB were found in the necrotic zone of the granulomas of INH- or CC-11050-alone treated animals (Fig. 3f and i) and none in the lesions of INH + CC-11050 treated rabbits (Fig. 3l).

3.6. Effect of CC-11050 Treatment on Immune Cell Function

To determine the extent of T cell activation, spleenocytes isolated from Mtb-infected rabbits that were untreated or drug treated, at 12 weeks post-infection, were stimulated with PPD, ConA or heat-killed Mtb, and their proliferative capacity was analyzed by CFSE dilution method using a flow cytometer as described previously (Subbian et al., 2011c). As shown in Fig. 4, in the absence of any antigen stimulation, the percent of proliferating $CD4^+$ T cells was significantly reduced in the CC-11050 (P = 0.033) or INH (P = 0.002) or INH + CC-11050 (P = 0.008) treated, compared to the untreated animals. Similar reductions in proliferating $CD4^+$ T cells were also noted between the untreated and treated animals, upon stimulation with heat-killed Mtb (P = 0.017 for CC-11050; P = 0.022 for INH; P = 0.008 for INH + CC-11050). In contrast to the proliferating $CD4^+$ T cells, no significant difference was observed in the percent of proliferating $CD8^+$ T cells between the untreated and different treatment groups (Supplementary Fig. 5) exposed ex vivo to the different antigens.

3.7. Global Lung Transcriptome of Mtb-infected Rabbits With or Without CC-11050 Treatment

To understand the effect of CC-11050 treatment on the host response in the lungs of Mtb-infected rabbits, we performed microarray-based global gene expression profiling analysis. Compared to the uninfected animals, 11,701 genes were significantly differentially expressed (SDEG; P < 0.05) in the Mtb-infected but untreated rabbit lungs at 12 weeks post-infection (Supplementary Fig. 6a). At this time, expression of 8701 genes was significantly affected in CC-11050 treated rabbit lungs, compared to the untreated animals. In addition, 4433 SDEG were commonly affected between the untreated and CC-11050 treated rabbit lungs. Among these common SDEG, expression of 1108 genes was up-regulated and 3325 were down-regulated in the untreated rabbit lungs, compared to 1114 up-regulated and 3319 down-regulated genes in CC-11050 treated animals (Supplementary Fig. 6b). The quality of microarray gene expression was validated by qPCR amplification of randomly selected host immune genes. As shown in Supplementary Table 4, the direction of expression of all tested genes as well as the level of expression of several genes were consistent between microarray and qPCR.

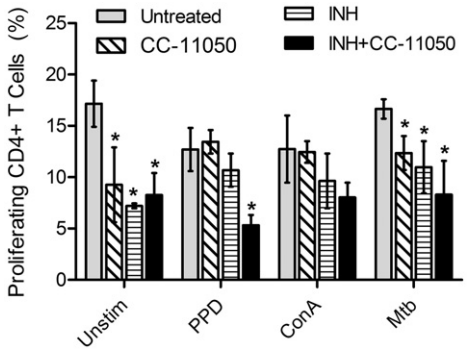

Fig. 4. Proliferative capacity of $CD4^+$ T cells. Percent of proliferating $CD4^+$ T cells in Mtb-infected untreated or CC-11050 or INH or INH + CC-11050 treated rabbits at 12 weeks post-infection (8 weeks treatment). Rabbit spleenocytes were either un-stimulated or stimulated with PPD, ConA or heat-killed Mtb before proliferation was measured by FACS analysis. Values plotted are average and standard deviation from 6 to 8 animals per group. *P < 0.05 compared to the untreated.

3.8. Gene Ontology Analysis of SDEG

To understand the biological functions, cell signaling networks and pathways that are affected by CC-11050 treatment, we performed gene ontology analysis on the SDEG from Mtb-infected untreated or CC-11050 treated rabbits, compared to the uninfected controls (Fig. 5). In the untreated rabbit lungs, genes associated with biological functions including inflammation, respiratory disease, lipid metabolism, cell compromise, infectious disease, immunological disease, small molecule transport, cell death and organismal injury were highly significantly enriched during Mtb infection. However, the significance of enrichment for most of these disease-associated functions, networks and pathways was less pronounced in the CC-11050 treated animals. Importantly, no significant enrichment of inflammatory response associated genes was noted in the CC-11050 treated rabbit lungs. Consistently, genes encoding for inflammatory molecules, including *GZMA*, *GZMB*, *FAM26F*, *MMP1*, *CXCL9*, *CXCL13*, *SLAMF7* were very highly up-regulated (>25 fold) and were among the top 10 most induced in the Mtb-infected untreated rabbit lungs (Supplementary Table 5). In contrast, except for *GZMA*, other genes were not significantly differentially expressed in the CC-11050 treated animals, compared to the uninfected animals.

3.9. CC-11050 Treatment Dampens Macrophage Activation and Inflammatory Response

To further elucidate the effect of CC-11050 treatment specifically on the host inflammatory response, we analyzed the expression profile of genes associated with the following networks: a) TNF-α regulation, b) macrophage activation and c) lung inflammation (Supplementary Fig. 7).

3.9.1. TNF-α Regulon Network

Among the SDEG, a subset of 205 genes in Mtb-infected rabbit lungs was associated with the regulation of TNF-α (Supplementary Fig. 7a and Supplementary Table 6). Of these, expression of 122 genes was up-regulated, including 31 genes expressed greater than 5-fold, and 83 were down-regulated in the untreated animals. In contrast, 50 genes were up-regulated, 47 genes were down-regulated and 108 genes were not significantly expressed in the CC-11050 treated rabbit lungs. In these animals, only 4 out of 50 genes were expressed to greater than 5-fold. Interestingly, 44 out of 50 up-regulated genes and 46 out of 47 down-regulated genes in CC-11050 treated rabbits were expressed in the same direction as the untreated, though the level of expression was lower in the CC-11050 treated group. Expression of *MCL1*, *CCL2*, *SMPDL3A* and *LOX* was down-regulated and *THY1* was up-regulated in the CC-11050 treated animals; these genes were expressed in the opposite direction in the untreated rabbit lungs (Supplementary Table 5).

3.9.2. Macrophage Activation Network

There were 68 genes associated with macrophage activation in Mtb-infected rabbit lungs at 12 weeks post-infection (Supplementary Fig. 7b and Supplementary Table 6). Among these, expression of 55 genes was up-regulated, including 15 genes induced to at least 5 fold. The number

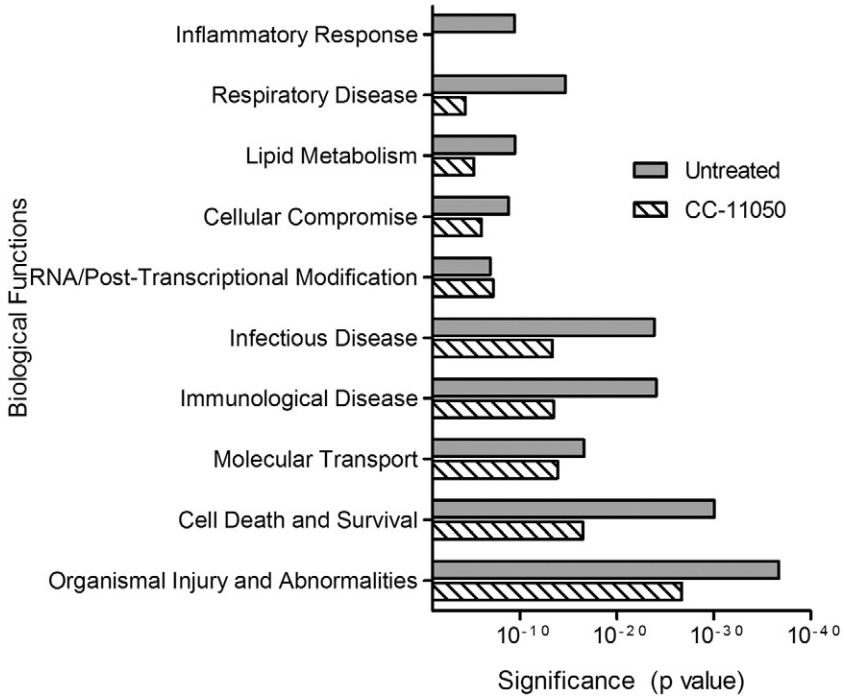

Fig. 5. Gene ontology analysis of significantly differentially expressed genes (SDEG) in Mtb-infected rabbit lungs. SDEG were selected based on 5% FDR and analyzed using Ingenuity Pathway Analysis (IPA) to determine enriched biological functions in the lungs of Mtb-infected untreated or CC-11050 treated rabbits at 12 weeks post-infection. Biological functions with a $P < 10^{-3}$ were considered significant. Inflammatory response network and pathways were not significantly enriched in the CC-11050 dataset.

of up-regulated genes was reduced by more than 50% (23 genes), with only 3 genes expressed to greater than 5 fold in the CC-11050 treated rabbit lungs. Expression of 20 out of 23 genes was in the same direction (up-regulated); while expression of *LCP1*, *CCL2* and *STAT3* was regulated in the opposite direction, between the untreated and CC-11050 treated rabbits (Supplementary Table 5). Though similar number of genes was down-regulated in the untreated (13 genes) and CC-11050 treated (12 genes) animals, expression of 23 genes was noted only in the former group.

3.9.3. Lung Inflammation Network

Of the 103 genes associated with lung inflammation, 65 genes were up-regulated and 38 genes were down-regulated in the untreated rabbit lungs (Supplementary Fig. 7c and Supplementary Table 6). Among the up-regulated genes, a subset of 22 genes was also up-regulated in CC-11050 treated animals. Similarly, 20 down-regulated genes in this group were also down-regulated in the untreated rabbits.

Twenty one SDEG were shared between the TNF-a regulon, macrophage activation and lung inflammation networks (Supplementary Fig. 8a and Supplementary Table 6). Of these, 18 genes were up-regulated and 3 genes were down-regulated in the untreated animals, compared to 6 up-regulated genes and 4 down-regulated genes in CC-11050 treated animals. Notably, expression of *TNF*, *CD14*, *IFNGR2*, *CD4*, *IL12B*, *IL16* and *CCL2* was highly up-regulated only in the untreated rabbits (Supplementary Fig. 8b and Supplementary Table 5). As shown in Supplementary Fig. 7, the expression of genes associated with TNF-α regulon, lung inflammation, macrophage activation and lung fibrosis

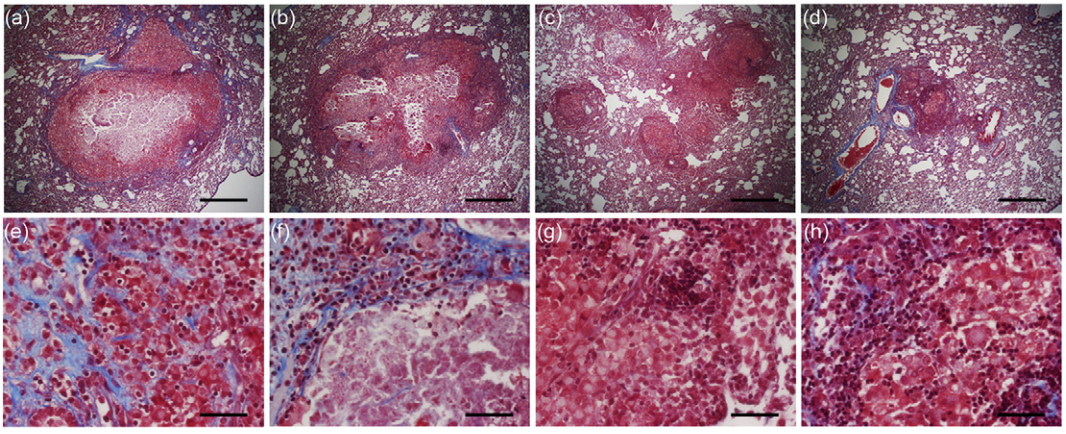

Fig. 6. Lung fibrosis in Mtb-infected rabbits with or without CC-11050 treatment at 12 weeks post infection. (a and e) Representative image of lung sections from Mtb infected untreated rabbits. Significant collagen deposition (blue staining) can be seen around the granulomas. (b and f) Representative image of lung sections from rabbits treated with INH alone. Significant collagen deposition (blue staining) surrounding the necrotic lesions can be seen in f. (c and g) Representative image of lung sections from rabbits treated with CC-11050 alone. Significantly less staining was observed in these granulomas. (d and h) Representative image of lung sections from rabbits treated with INH + CC-11050. Minimal amount of fibrosis can be visualized surrounding the granuloma in h. All sections were stained using Masson's trichrome method. Images a–d were photographed at 4× (Scale bar = 500 μm) and e–h at 40× magnification (Scale bar = 50 μm), respectively.

was similar between CC-11050 and CC-3052, treated rabbit lungs (Supplementary Fig. 9).

3.10. CC-11050 Treatment Affects Lung Fibrosis

To evaluate the effect of CC-11050 on the extent of the fibrotic process, lung sections from all treated and untreated infected rabbits were stained using Masson's trichrome method, specific for fibrosis, collagen deposition and tissue remodeling (Fig. 6). Microscopic examination revealed little to no fibrosis in the lungs at 4 or 8 weeks post-infection (not shown). At 12 weeks post-infection, significant collagen deposition (blue staining) was observed around the granulomas and adjacent to the necrotic area in the lungs of control untreated Mtb-infected animals (Fig. 6a and e). Based on the Ashcroft scoring system the average value was 2.8. Similarly, extensive fibrosis was seen in the lungs of animals treated with INH alone (Fig. 6b and f) (Ashcroft score — 2.7). In contrast, the lungs of animals treated with CC-11050 alone (Fig. 6c and g) contained granulomas with almost no fibrosis (Aschroft score — 0.8) and INH + CC-11050 treated rabbit lungs (Fig. 6d and h) had very minimal amounts of fibrosis, with an average score of 0.5. These findings demonstrate that eight weeks of treatment with the CC-11050 or the combination of CC-11050 and INH resulted in diminished infection-induced fibrosis around and within lung lesions.

3.11. Modulation of Lung Fibrosis and Wound Healing Network by CC-11050 Treatment

Since histologic staining showed diminished fibrosis in CC-11050 treated, compared to the untreated rabbit lungs, we investigated the transcriptional profile of lung fibrosis and wound healing network genes at 12 weeks post-infection. Of the SDEG, a subset of 59 genes was associated with the lung fibrosis network (Fig. 7a and Supplementary Table 6). While expression of 36 genes (61%) was up-regulated and 23 genes were down-regulated in the untreated, only 11 genes were up-regulated and 7 genes were down-regulated in the CC-11050 treated rabbit lungs. In the later group of animals, 41 genes (69%) were not significantly expressed. To further elucidate the expression pattern of genes involved in tissue remodeling, we performed qPCR on selected host genes that code for collagenase (*MMP1*), gelatinase (*MMP2*), elastase (*MMP12*) and membrane-type (*MMP14*) matrix metalloproteases and a matrix proteoglycan, decorin (*DCN*) (Fig. 7b). Compared to the Mtb-infected untreated animals, expression of *MMP1*, *MMP12*, *MMP14* and *DCN* was significantly reduced ($P < 0.05$) in the CC-11050 treated rabbit lungs at 12 weeks post-infection (8 weeks of treatment). In addition, *MMP12* was significantly reduced in the INH + CC-11050 treated group, compared to the untreated rabbits. No significant difference was observed between INH treated versus untreated rabbit lungs for any of the tested genes. Taken together, our qPCR results are consistent with and support the histologic finding of reduced fibrosis in CC-11050 treated rabbit lungs.

4. Discussion

Host-directed therapy is being actively pursued as an alternate strategy to cure TB.

In this study, we found that coupling INH therapy with adjunctive PDE4i CC-11050 treatment significantly reduced the bacillary burden and tissue inflammation and improved lung pathology in Mtb-infected rabbits. Consistently, lung fibrosis was significantly reduced in the CC-11050 treated animals. Lung transcriptome analyses revealed dampening of the expression of genes associated with TNF-α, macrophage activation and lung inflammation networks. Our results strongly suggest that CC-11050 can be used as an adjunct therapeutic molecule to improve the outcome of antibiotic treatment in patients with pulmonary TB.

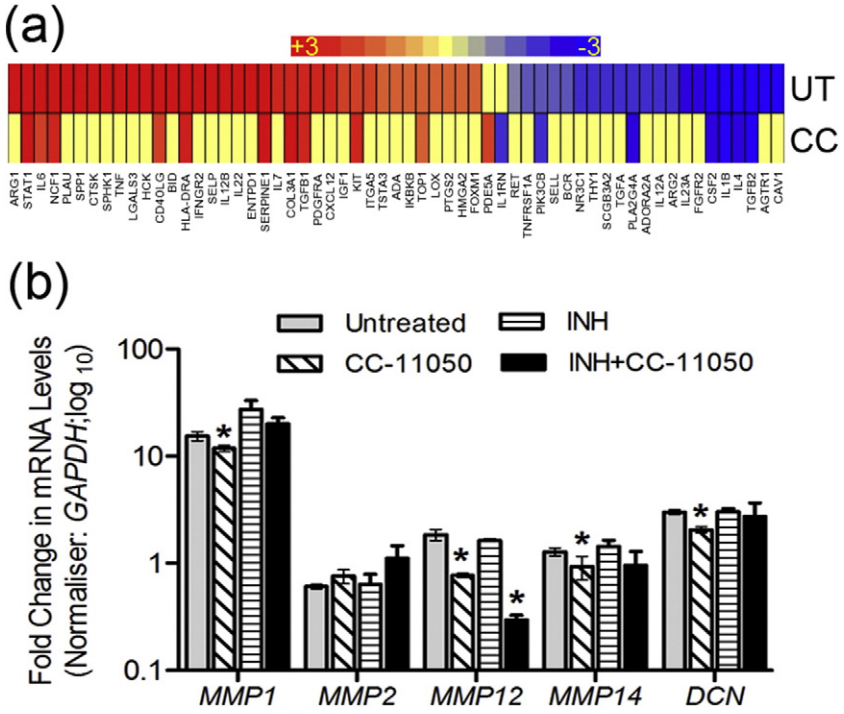

Fig. 7. Expression profile of lung fibrosis network genes in Mtb-infected rabbits with or without CC-11050 treatment. (a) Intensity plot of SDEG associated with lung fibrosis network in Mtb-infected untreated (UT) or CC-11050 treated (CC) rabbit lungs at 12 weeks post-infection. Red color indicates up-regulated genes; blue color represents down-regulated genes and intensity of color denotes relative level of respective gene expression. The scale bar ranges from +3 (red) to −3(blue). Individual genes in this network and their expression levels are shown in Supplementary Table 5. (b) qPCR analysis of selected genes involved in fibrosis and tissue remodeling in the lungs of Mtb-infected untreated (UT) or CC-11050 treated (CC) rabbits at 12 weeks post-infection. *$P < 0.05$ compared to the untreated.

Taken together, these results validate our central hypothesis that dampening the host inflammatory response by down-regulating TNF-α through PDE4 inhibition therapy can improve the outcome of antibiotic treatment during Mtb infection. In contrast, in a recent mouse model of Mtb infection, treatment with rolipram and cilomilast, two FDA approved PDE4i used for the treatment of depression and COPD respectively, in combination with anti-TB drugs did not show significant improvement in disease or reducing the bacillary load (Maiga et al., 2013). This difference between the published study and our work might reflect the different enzyme specificities of these three PDE4i. The PDE4 family has at least 4 subtypes (PDE4A-4D) and at least 15 isotypes that are differentially localized and expressed among the host immune cells (Houslay & Adams, 2003). In vitro, rolipram inhibits PDE4A, 4B and 4D activities, with higher and similar inhibitory activity towards PDE4B and 4D (MacKenzie & Houslay, 2000). It is likely that the specific PDE4 isoforms targeted by CC-11050 differ from those targeted by rolipram. In addition, unlike the rabbit, the standard mouse model of pulmonary Mtb infection does not recapitulate the pathologic sequence of TB manifestations found in humans, such as necrosis, hypoxic lesions and cavitation (Gupta & Katoch, 2005; O'Toole, 2010). Since the effect of immune modulators on TB pathology and associated host gene expression varies significantly between murine and rabbit models, the results obtained in the two models cannot be directly comparable In addition, the divergent results between the current study and a report by Maiga et al. (2013) may be due to the difference in the treatment regimen (single-versus multi-drug combinatorial therapy).

A critical observation in this study is the reduced lung fibrosis during CC-11050 treatment of Mtb-infected rabbits. One of the hallmarks of advanced pulmonary TB in humans is the extensive tissue damage due to cavities that are surrounded by thick fibrosis (Kaplan et al., 2003; Subbian et al., 2015). Although tissue remodeling during fibrosis aids in the stabilization and healing of granulomas with caseation, extensive fibrosis resulting in tissue scarring, significantly reduces lung function (Hunter, 2011a; Hunter, 2011b). In addition, granulomas with fibrosis and extensive tissue remodeling have poor drug penetration and accumulation resulting in poor bactericidal activity by the anti-TB drugs (Kjellsson et al., 2012). Moreover, Mtb can thrive in a fibrotic lesion and can be reactivated during immune suppression (Paige & Bishai, 2010).

Matrix metalloproteases (MMPs) are a family of cellular matrix degrading nucleases that play a central role in tissue remodeling and fibrosis during pulmonary cavitary TB in humans and in relevant animal models; small molecules that can interfere with MMP signaling have been suggested as immunomodulatory drugs for TB treatment (Ong et al., 2014; Elkington et al., 2011; Dharmadhikari & Nardell, 2008). In general, induction of several MMPs, including MMP1, MMP12 and MMP14 correlates with disease severity, tissue destruction and inflammation during active TB in humans and in the non-human primates and rabbit models of pulmonary TB (Subbian et al., 2011b; Subbian et al., 2015; Ong et al., 2014; Kim et al., 2010; Mehra et al., 2010). Consistent with these findings, we observed up-regulation of *MMP1*, 12, 14 and *DCN* in Mtb-infected untreated rabbit lungs associated with increased fibrosis around the granulomas. We postulate that in the CC-11050 + INH treated rabbits, significant down-regulation of these MMPs, concomitant with a dampened inflammatory response, contributes to reduced fibrosis, and that this facilitates improved accessibility of antibiotics and improved bacterial killing. We believe that these findings can provide a rationale for developing CC-11050 as an adjunctive agent in TB therapy.

Funding Sources

This study was funded by a grant from NIH-NIAID to GK (AI054338) and to SS (1R21AI110335-01) and by a New Jersey Health Foundation award to SS. The funding agencies do not have any role in the study design, data collection, analysis or interpretation of results or writing the manuscript or the decision to submit it for publication.

Conflict of Interest Statement

VK and JBZ are employees of Celgene Corporation. GK is a member of the Board of Celgene Corporation. All other authors: none to declare.

Author Contributions

SS, JBZ and GK conceived the study and designed the experiments. SS, LT, JH, BP and POB performed the experiments. VD supervised the PK-PD studies. SS, LT, VD, VK, JBZ and GK analyzed and interpreted the data. All the authors have read and edited the manuscript.

Appendix A. Supplementary Data

Supplementary data to this article can be found online at http://dx.doi.org/10.1016/j.ebiom.2016.01.015.

References

Mitchison, D.A., 2000. Role of individual drugs in the chemotherapy of tuberculosis. Int J. Tuberc. Lung Dis. 4, 796–806.
Sirgel, F.A., Donald, P.R., Odhiambo, J., Githui, W., Umapathy, K.C., et al., 2000. A multicentre study of the early bactericidal Activity of anti-tuberculosis drugs. J. Antimicrob. Chemother. 45, 859–870.
Zhang, Y., Yew, W.W., Barer, M.R., 2012. Targeting persisters for tuberculosis control. Antimicrob. Agents Chemother. 56, 2223–2230.
Cardona, P.J., 2010. Revisiting the natural history of tuberculosis. The inclusion of constant reinfection, host tolerance, and damage-response frameworks leads to a better understanding of latent infection and its evolution towards active disease. Arch. Immunol. Ther. Exp. 58, 7–14.
Ehlers, S., 2009. Lazy, dynamic or minimally recrudescent? On the elusive nature and location of the *Mycobacterium* responsible for latent tuberculosis. Infection 37, 87–95.
den Boon, S., Verver, S., Lombard, C.J., Bateman, E.D., Irusen, E.M., et al., 2008. Comparison of symptoms and treatment outcomes between actively and passively detected tuberculosis cases: the additional Value of active case finding. Epidemiol. Infect. 136, 1342–1349.
Verver, S., Warren, R.M., Beyers, N., Richardson, M., van der Spuy, G.D., et al., 2005. Rate of reinfection tuberculosis after successful treatment is higher than rate of new tuberculosis. Am. J. Respir. Crit. Care Med. 171, 1430–1435.
Zumla, A.I., Gillespie, S.H., Hoelscher, M., Philips, P.P., Cole, S.T., et al., 2014. New antituberculosis drugs, regimens, and adjunct therapies: needs, advances, and future prospects. Lancet Infect. Dis. 14, 327–340.
Dorhoi, A., Kaufmann, S.H., 2014. Perspectives on host adaptation in response to *Mycobacterium tuberculosis*: modulation of inflammation. Semin. Immunol. 26, 533–542.
Behar, S.M., Carpenter, S.M., Booty, M.G., Barber, D.L., Jayaraman, P., 2014. Orchestration of pulmonary T cell immunity during *Mycobacterium tuberculosis* infection: immunity interruptus. Semin. Immunol. 26, 559–577.
Kaufmann, S.H., Dorhoi, A., 2013. Inflammation in tuberculosis: interactions, imbalances and interventions. Curr. Opin. Immunol. 25, 441–449.
Sugawara, I., 2009. Why does tuberculosis lead to specific inflammation? Nihon Hansenbyo Gakkai Zasshi 78, 263–269.
Schlesinger, L.S., 1996. Role of mononuclear phagocytes in *M. tuberculosis* pathogenesis. J. Investig. Med. 44, 312–323.
Chao, M.C., Rubin, E.J., 2010. Letting sleeping dos lie: does dormancy play a role in tuberculosis? Annu. Rev. Microbiol. 64, 293–311.
Wallis, R.S., Hafner, R., 2015. Advancing host-directed therapy for tuberculosis. Nat. Rev. Immunol. 15, 255–263.
Hawn, T.R., Shah, J.A., Kalman, D., 2015. New tricks for old dogs: countering antibiotic resistance in tuberculosis with host-directed therapeutics. Immunol. Rev. 264, 344–362.
Francis, S.H., Blount, M.A., Corbin, J.D., 2011. Mammalian cyclic nucleotide phosphodiesterases: molecular mechanisms and physiological functions. Physiol. Rev. 91, 651–690.
Conti, M., Richter, W., Mehats, C., Livera, G., Park, J.Y., et al., 2003. Cyclic AMP-specific PDE4 phosphodiesterases as critical Components of cyclic AMP signaling. J. Biol. Chem. 278, 5493–5496.
Keravis, T., Lugnier, C., 2012. Cyclic nucleotide phosphodiesterase (PDE) isozymes as targets of the intracellular signalling network: benefits of PDE inhibitors in various diseases and perspectives for future therapeutic developments. Br. J. Pharmacol. 165, 1288–1305.
Bender, A.T., Beavo, J.A., 2006. Cyclic nucleotide phosphodiesterases: molecular regulation to clinical use. Pharmacol. Rev. 58, 488–520.
Spina, D., 2003. Phosphodiesterase-4 inhibitors in the treatment of inflammatory lung disease. Drugs 63, 2575–2594.
Houslay, M.D., Sullivan, M., Bolger, G.B., 1998. The multienzyme pde4 cyclic adenosine monophosphate-specific phosphodiesterase family: intracellular targeting, regulation, and selective inhibition by compounds exerting anti-inflammatory and antidepressant actions. Adv. Pharmacol. 44, 225–342.
Azam, M.A., Tripuraneni, N.S., 2014. Selective phosphodiesterase 4B inhibitors: a review. Sci. Pharm. 82, 453–481.
Maurice, D.H., Ke, H., Ahmad, F., Wang, Y., Chung, J., et al., 2014. Advances in targeting cyclic nucleotide phosphodiesterases. Nat. Rev. Drug Discov. 13, 290–314.

Moreira, A.L., Tsenova-Berkova, L., Wang, J., Laochumroonvorapong, P., Freeman, S., et al., 1997. Effect of cytokine modulation by thalidomide on the granulomatous response in murine tuberculosis. Tuber. Lung Dis. 78, 47–55.
Tsenova, L., Mangaliso, B., Muller, G., Chen, Y., Freedman, V.H., et al., 2002. Use of IMiD3, a thalidomide analog, as an adjunct to therapy for experimental tuberculous meningitis. Antimicrob. Agents Chemother. 46, 1887–1895.
Koo, M.S., Manca, C., Yang, G., O'Brien, P., Sung, N., et al., 2011. Phosphodiesterase 4 inhibition reduces innate immunity and improves isoniazid clearance of *Mycobacterium tuberculosis* in the lungs of infected mice. PLoS One 6, e17091.
Subbian, S., Tsenova, L., O'Brien, P., Yang, G., Koo, M.S., et al., 2011a. Phosphodiesterase-4 inhibition alters gene expression and improves isoniazid-mediated clearance of *Mycobacterium tuberculosis* in rabbit lungs. PLoS Pathog. 7, e1002262.
Subbian, S., Tsenova, L., O'Brien, P., Yang, G., Koo, M.S., et al., 2011b. Phosphodiesterase-4 inhibition combined with isoniazid treatment of rabbits with pulmonary tuberculosis reduces macrophage activation and lung pathology. Am. J. Pathol. 179, 289–301.
Subbian, S., Tsenova, L., Yang, G., O'Brien, P., Parsons, S., et al., 2011c. Chronic pulmonary cavitary tuberculosis in rabbits: a failed host immune response. Open Biol. 1, 110016.
Tsenova, L.H.R., Ellison, E., Manca, C., Kaplan, G., 2006. Aerosol exposure system for rabbits: application to *M. tuberculosis* infection. Appl. Biosaf. 11, 7–14.
Subbian, S., Tsenova, L., O'Brien, P., Yang, G., Kushner, N.L., et al., 2012. Spontaneous latency in a rabbit model of pulmonary tuberculosis. Am. J. Pathol. 181, 1711–1724.
Hubner, R.H., Gitter, W., El Mokhtari, N.E., Mathiak, M., Both, M., et al., 2008. Standardized quantification of pulmonary fibrosis in histological samples. Biotechniques 44 (507–511), 507–514.
Robbe, A., Tassin, A., Carpentier, J., Decleves, A.E., Mekinda Ngono, Z.L., et al., 2015. Intratracheal bleomycin aerosolization: the best route of administration for a scalable and homogeneous pulmonary fibrosis rat model? Biomed. Res. Int. 2015, 198418.
Subbian, S., O'Brien, P., Kushner, N.L., Yang, G., Tsenova, L., et al., 2013a. Molecular immunologic correlates of spontaneous latency in a rabbit model of pulmonary tuberculosis. Cell Commun. Signal. 11, 16.
Subbian, S., Bandyopadhyay, N., Tsenova, L., O'Brien, P., Khetani, V., et al., 2013b. Early innate immunity determines outcome of *Mycobacterium tuberculosis* pulmonary infection in rabbits. Cell Commun. Signal. 11, 60.
Maiga, M., Ammerman, N.C., Maiga, M.C., Tounkara, A., Siddiqui, S., et al., 2013. Adjuvant host-directed therapy with types 3 and 5 but not type 4 phosphodiesterase inhibitors shortens the duration of tuberculosis treatment. J. Infect. Dis. 208, 512–519.
Houslay, M.D., Adams, D.R., 2003. PDE4 cAMP Phosphodiesterases: Modular Enzymes That Orchestrate Signalling Cross-Talk, Desensitization and Compartmentalization. Biochem. J. 370, 1–18.
MacKenzie, S.J., Houslay, M.D., 2000. Action of rolipram on specific PDE4 cAMP phosphodiesterase isoforms and on the phosphorylation of cAMP-response-element-binding protein (CREB) and p38 mitogen-activated protein (MAP) kinase in U937 monocytic cells. Biochem. J. 347, 571–578.
Gupta, U.D., Katoch, V.M., 2005. Animal Models of Tuberculosis. Tuberculosis (Edinb.) 85, 277–293.
O'Toole, R., 2010. Experimental models used to study human tuberculosis. Adv. Appl. Microbiol. 71, 75–89.
Kaplan, G., Post, F.A., Moreira, A.L., Wainwright, H., Kreiswirth, B.N., et al., 2003. *Mycobacterium tuberculosis* growth at the cavity surface: a microenvironment with failed immunity. Infect. Immun. 71, 7099–7108.
Subbian, S., Tsenova, L., Kim, M.J., Wainwright, H.C., Visser, A., et al., 2015. Lesion-specific immune response in granulomas of patients with pulmonary tuberculosis: a pilot study. PLoS One 10, e0132249.
Hunter, R.L., 2011a. On the pathogenesis of post primary tuberculosis: the role of bronchial obstruction in the pathogenesis of cavities. Tuberculosis (Edinb.) 91 (Suppl. 1), S6–S10.
Hunter, R.L., 2011b. Pathology of post primary tuberculosis of the lung: an illustrated critical review. Tuberculosis (Edinb.) 91, 497–509.
Kjellsson, M.C., Via, L.E., Goh, A., Weiner, D., Low, K.M., et al., 2012. Pharmacokinetic evaluation of the penetration of antituberculosis agents in rabbit pulmonary lesions. Antimicrob. Agents Chemother. 56, 446–457.
Paige, C., Bishai, W.R., 2010. Penitentiary or penthouse condo: the tuberculous granuloma from the microbe's point of view. Cell. Microbiol. 12, 301–309.
Ong, C.W., Elkington, P.T., Friedland, J.S., 2014. Tuberculosis, pulmonary cavitation, and matrix metalloproteinases. Am. J. Respir. Crit. Care Med. 190, 9–18.
Elkington, P., Shiomi, T., Breen, R., Nuttall, R.K., Ugarte-Gil, C.A., et al., 2011. MMP-1 drives immunopathology in human tuberculosis and transgenic mice. J. Clin. Invest. 121, 1827–1833.
Dharmadhikari, A.S., Nardell, E.A., 2008. What animal models teach humans about tuberculosis. Am. J. Respir. Cell Mol. Biol. 39, 503–508.
Kim, M.J., Wainwright, H.C., Locketz, M., Bekker, L.G., Walther, G.B., et al., 2010. Caseation of human tuberculosis granulomas correlates with elevated host lipid metabolism. EMBO Mol. Med. 2, 258–274.
Mehra, S., Pahar, B., Dutta, N.K., Conerly, C.N., Philippi-Falkenstein, K., et al., 2010. Transcriptional reprogramming in nonhuman primate (rhesus macaque) tuberculosis granulomas. PLoS One 5, e12266.